SDSU STRUCTURAL ENGINEERING RESEARCH PROJECT

Report No. SERP – 23/03

March 2023

Reconnaissance Report of Observed Structural Bridge Damage

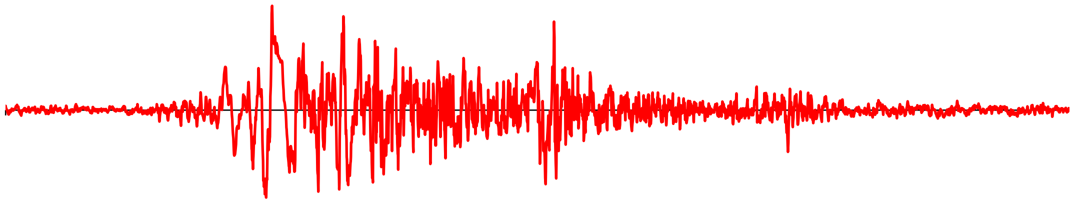

M_w 7.8 Turkiye (Turkey) Earthquake of 2023

by

Robert K. Dowell, Ph.D., P.E.[1]

[1]Professor and Principal Investigator

Department of Civil, Construction, and Environmental Engineering
College of Engineering
San Diego State University
San Diego, California

1. Introduction

On February 6, 2023, a M_w 7.8 earthquake [1] occurred at 4:17 am (local time) in southern Turkiye (Turkey) followed by a M_w 7.5 earthquake [2] in the same general region about 9 hours later, at 1:24 pm (local time), with strike-slip fault rupture lengths of 180 miles (290 km) [3] and 99 miles (160 km) [4], respectively. The result of this unprecedented series of back-to-back earthquakes, in populated regions, was widespread structural damage and failures, and related loss of life, with tens of thousands of collapsed buildings over multiple cities as well as rural areas of southern Turkiye and northern Syria, and approximately 50,000 people killed in the collapsed structures based on the number of bodies pulled from the rubble. About 350,000 individual apartments in Turkiye alone were destroyed, often having multiple people living in them, indicating that the actual death toll may be many times higher than the official one. The number of structural failures and associated extreme loss of life, as well as economic losses of tens of billions of dollars (in US currency), makes this the worst earthquake disaster in Turkiye's history and, possibly, in human history.

While the second earthquake is not considered an aftershock of the M_w 7.8 event, since it occurred on a separate fault line, the intense shaking from the first event and redistribution of strains and stresses throughout the complex of faults in this area of southern Turkiye almost certainly caused the second earthquake to happen, suddenly releasing all of its stored potential strain energy. The widespread shaking and destruction from these two earthquakes can be attributed to the two separate faults being approximately perpendicular to each other, with the second one starting near the end of the first one that slipped. While severe ground shaking was felt in southern Turkiye and northern Syria, the epicenters and extents of both fault ruptures were entirely in Turkiye.

The structural engineering reconnaissance team (called the team from hereon) arrived at their base in Adana, southern Turkiye, two weeks after the earthquake sequence, with the first day of field visits scheduled for February 20th. This was just after search and rescue efforts had completed, and before most of the damaged and failed structures had been demolished and removed. On the evening of February 20th, when back in Adana after the first day in the field, the team experienced the largest of the 1000s of aftershocks from the two earthquakes, which collapsed a few more buildings close to the epicenter. This M_w 6.3 aftershock occurred at 7:04 pm (local time) near Antakya (Antioch) in Hatay Province, about 70 miles from Adana, resulting in the team feeling reduced shaking than at the epicenter.

The team visited damaged and failed structures in a total of three ways; the first was based on knowledge ahead of time about a particular structure that was damaged, followed by determining how to get there and obtaining permission to visit the structure from local authorities. The second was just happening to see a particular structure of interest (with or without visible damage) from the vehicle as the team was driving in, or toward, the affected regions, and then stopping to inspect it. Looking out the windows as the reconnaissance van drove along, multiple damaged and failed buildings, silos, mosques, churches and industrial buildings were seen, as well as damaged bridges. The team had a hired driver for the vehicle, allowing all of the members to look out the windows when traveling from region-to-region, especially as more failed structures became apparent as the van approached the most affected areas. A third way to visit a series of structures was on foot, when in a very dense area of damaged and collapsed structures.

From Adana (where about 10 buildings had collapsed two weeks prior from the earthquake sequence), the team went to the field each day for six days in a row to different towns, cities and regions, sometimes to more than one in the same day, returning to Adana each evening. Drive times ranged from one to three hours, each way, depending on where the team was going. Towns, cities and regions visited include Iskenderun, Antakya (Antioch), Osmaniye, Kahramanmaras, Gaziantep, Nurdagi, Golbasi and Hatay. A couple of buildings in Adana, where the team stayed, were also inspected. Residential buildings, industrial buildings, bridges, mosques, churches and schools were visited and inspected for damage. While bridge structures were damaged, as expected and designed for from such a major event, the team does not know of any that collapsed; since they are state-owned, bridges are designed and built to a higher engineering standard than residential buildings, which are privately owned.

It appears that the typical building type used in Turkiye for residential structures of a reinforced concrete (RC) frame of columns and girders with infill walls, made from bricks or masonry blocks, is the primary cause for so many building collapses and deaths. The infill walls but-up against the frame members, with no gaps, causing these walls to take the majority of the lateral loads from an earthquake until they fail in shear from in-plane loading, and then fall out from the perpendicular direction of loading, with shaking in both horizontal directions (EW and NS) occurring simultaneously throughout the earthquake. Column members were seen to be pushed out and failed by these stiff infill walls since no gaps were provided, preventing the columns to properly flex in bending, as expected in design.

The bricks, or masonry blocks, are not tied to the frame or to each other, resulting in nothing to prevent them popping out, causing falling hazards for people and property below the buildings, as well as inside the apartments, and a changed response of the building as the earthquake continues. Since the infill walls are not properly tied to the frame of the building, they are not considered in the design of these structures. However, as the crisscross diagonal shear cracks clearly attest to in most of these damaged and failed structures, at almost all infill walls, these walls *are* initially resisting the lateral earthquake loads, regardless if they were not considered in the design. Once the walls fully, or partially, fall out, then the remaining RC frame is suddenly tasked with taking the earthquake loads, with much longer periods and a changed response. Prior to this, a building attracts much more load than expected in design due to the stiffer response from the combined frame and infill walls than the frame acting alone, with higher amplification for the short-period structure overloading the frame once the infill walls are gone. Lack of good detailing in expected plastic hinge regions also contributed to building failures. In some regions, liquefaction was also a cause of structural damage and failures, with the team observing sand boils, lateral spreading and settlement.

As Turkiye rebuilds, it must consider changes to this type of residential construction. Perhaps base isolation can be used for all new buildings, as well as for seismic retrofitting of older structures. Base isolation essentially decouples the structure from the ground, reducing structural accelerations and forces to a level that, perhaps, not a single building would have collapsed from these two earthquakes had they been base-isolated, significantly reducing the number of people killed. Base isolation does not have to be expensive, and could be used to mitigate future earthquake damage across Turkiye, including in Istanbul where about 15 million people live and now fear a large earthquake there. This report is dedicated to those who lost their lives in Turkiye and Syria, from what may be the worst earthquake disaster in human history, and to the civil engineers who will design and build new structures, as well as seismically retrofit existing ones, that will not collapse in future earthquakes in Turkiye and around the world.

While the team is writing a report that includes all of the structures that were inspected, this report considers only bridge structures. The author has over 30 years of experience in bridge design, structural analysis and physical testing to failure in the laboratory. The opinions expressed in this report are his alone.

2. Bridge Discussion

It is significant that tens of thousands of buildings collapsed in southern Turkiye from the sequential M_w 7.8 and M_w 7.5 earthquake events and, as far as the team knows, not a single bridge structure collapsed, although some were heavily damaged, which is expected and designed for in such a large event. Bridge structures have collapsed from smaller earthquakes in California than those just experienced in southern Turkiye, such as from the M_w 6.6 1971 San Fernando earthquake [5], M_w 6.9 1989 Loma Prieta earthquake [6], and the M_w 6.7 1994 Northridge earthquake [7]. In some instances the bridge structures that failed in past California earthquakes were over 100 miles (161 km) from the epicenter. Perhaps bridges did not collapse in southern Turkiye because Turkiye has been keeping up with the most recent seismic bridge design specifications from California [8], and elsewhere, that improve from lessons learned after each major earthquake.

This revelation that no bridges collapsed from the earthquake sequence in southern Turkiye was from (1) the team's own observations of more than 10 bridges that were inspected, as well as ones that were driven past and over while traveling from town-to-town in the affected areas of southern Turkiye, and (2) multiple meetings and discussions with Turkish professionals and people living in Turkiye. It is probable that this is because buildings are typically private ventures while bridges are state-sponsored. Thus bridges were, for the most part, designed and built to modern specifications for earthquake response while buildings often were not, even though current Turkish building seismic design specifications [9] are essentially identical to US and Western standards. Hence, while this was a natural disaster it is clearly also a man-made disaster. While none of the bridge structures had collapsed by the time of the inspections, there are several bridges that had unusual and/or severe damage from the M_w 7.8 earthquake.

Three of the bridges with the most interesting and significant observed damage are presented herein. Bridge 1 formed a plastic hinge 25% up the column height, with vertical rebar buckling and transverse rebar yielding clearly visible, while Bridge 2 has significantly damaged girder ends, with no concrete remaining – just the rebar cage. And, yet, traffic is still flowing across both of these bridges. It is expected that multiple span collapses will happen soon at Bridge 2 from a combination of earthquake aftershocks and repeated live loading, and should be closed to vehicular traffic. Bridge 1 is a major structure on a busy highway, and should be assessed by the bridge design group in Turkiye. Future aftershocks could cause a few more nonlinear cycles and failure of the column plastic hinge, resulting in complete collapse of the bridge structure. But other than some minor damage at the abutments, the rest of Bridge 1 appears to be in good condition. A seismic retrofit to the plastic hinge region, or entire column, could save this structure. Because the vertical steel has buckled, in addition to increasing the lateral confinement to the plastic hinge, new vertical steel would have to be added. Bridge 3 had damage to the girder ends as well as to interior and exterior shear keys at the abutments and bents.

Detailed structural analyses have not so far been conducted for the bridge structures of interest because (1) of time constraints for this reconnaissance report and (2) the bridge plans have not yet been obtained from Turkiye. Therefore, the presentation in this report is of observed structural bridge damage and possible explanations for how the damage developed, as well as the level of shaking each bridge experienced based on nearby strong motion station measurements. It is hoped that in the near future the plans for these bridges will be obtained which, in conjunction with the measured ground motions near the three bridges, will allow nonlinear time-history analyses to be conducted, as well as the simpler pushover and spectral analyses, in order to better understand the significant and, in several cases, unusual damage observed.

GPS north and east coordinates, as well as elevations, were determined at the three bridge sites from a Garmin 64S hand-held GPS device (Fig. 2-1), allowing the closest free-field strong ground motion station to be found for each bridge, as well as the distances from the bridges to each earthquake epicenter. Bridge 1 was only 18.1 miles (29.2 km) from the epicenter of the M_w 7.8 earthquake, while Bridge 2 was 80.8 miles (130 km) away and Bridge 3 was 81.4 miles (131 km) away. For the M_w 7.5 earthquake, the distances from the epicenter to the three bridges were 64.9 miles (104 km) for Bridge 1 and 134 miles (216 km) for both Bridges 2 and 3. Since all three bridges were significantly closer to the epicenter of the M_w 7.8 earthquake than for the M_w 7.5 earthquake, and because it was the initial and larger event, only the M_w 7.8 earthquake is considered in detail in this report.

Fig. 2-1. Garmin GPS Unit used in the field to determine coordinate location of bridges inspected for damage

3. Measured Free-field Ground Motions near Bridge Structures

Station 2712 was the closest strong motion station to Bridge 1 - 2.00 miles (3.21 km) away. Free-field ground accelerations from Station 2712 during the M_w 7.8 earthquake in the horizontal East-West (EW) and North-South (NS) directions are given in Figs. 3-1a and b, respectively. Peak horizontal ground accelerations (PGA) are 0.607 g for the EW direction and 0.565 g in the NS direction, with PGA of 0.354 g in the vertical direction, as seen in Fig. 3-1c. The 5%-damped spectral acceleration graphs for the EW and NS directions are given in Fig. 3-2a, with maximum values of 1.83 g and 1.90 g, respectively. Also shown in Fig. 3-2a is the smoothed Caltrans, 5%-damped bridge design spectral curve for a M_w 8 earthquake (plus or minus M_w 0.25) having PGA of 0.7 g and a rock or stiff soil profile [10], with maximum value of 1.82 g. This Caltrans design curve was obtained from an earlier version of the Caltrans Seismic Design Specifications (SDC) [10] since the latest version of the SDC [8] does not have such a graph readily available for stiff soil and rock sites. Vertical spectral accelerations are given in Fig. 3-2b, with maximum value of 1.37 g.

Station 3124 was the closest strong motion station to both Bridges 2 and 3 at 2.14 miles (3.44 km) from Bridge 2 and 2.33 miles (3.75 km) from Bridge 3. Recorded accelerations versus time at this station from the M_w 7.8 earthquake are given in Figs. 3-3a and b for the horizontal EW and NS directions, respectively. PGAs are 0.659 g in the EW direction and 0.581 g in the NS direction, as seen in Figs. 3-3a and b. In the vertical direction the PGA was 0.589 g (Fig. 3-3c). Acceleration spectra results with 5% damping are given in Fig. 3-4a for the two horizontal directions as well as the Caltrans bridge design curve for M_w 8. The vertical direction spectrum is given in Fig. 3-4b. By comparing the horizontal acceleration spectra developed from ground motions measured at Station 3124 to the smoothed Caltrans bridge design acceleration spectrum for M_w 8 and PGA of 0.7 g at a rock or stiff soil site, it is clear that Station 3124 must have a deep layer of soft soil beneath it (or soft soil from the earthquake epicenter to the station) for the peak spectral responses to shift to such long natural structural periods (Fig. 3-4a). This is seen in both EW and NS directions.

Therefore, Bridges 2 and 3 are probably on deep, soft soil. In the EW direction the maximum spectral acceleration of 2.15 g (Fig. 3-4a) was greater than the maximum value of 1.82 g from the smoothed Caltrans design curve for M_w 8 earthquakes (Fig. 3-4a), demonstrating the intense level of shaking that occurred at Bridges 2 and 3. For the NS direction, the maximum spectral value was 1.44 g (Fig. 3-4a). In the vertical direction, the peak spectral acceleration was 1.64 g, which is important as it implies that the precast girders of both Bridges 2 and 3 lifted off of their simple supports and slammed back down, multiple times, significantly contributing to the observed damage discussed below for both of these bridges, especially for Bridge 2.

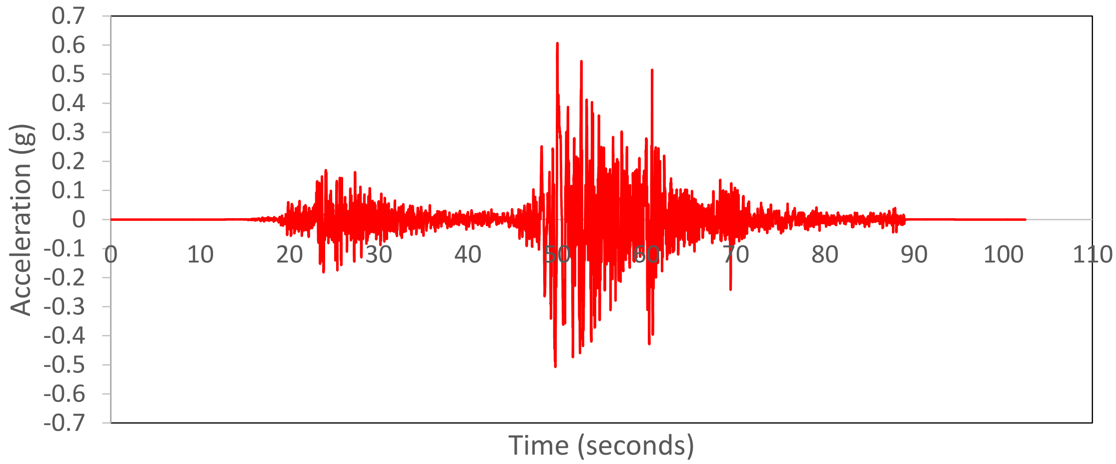

(a) EW direction accelerations versus time

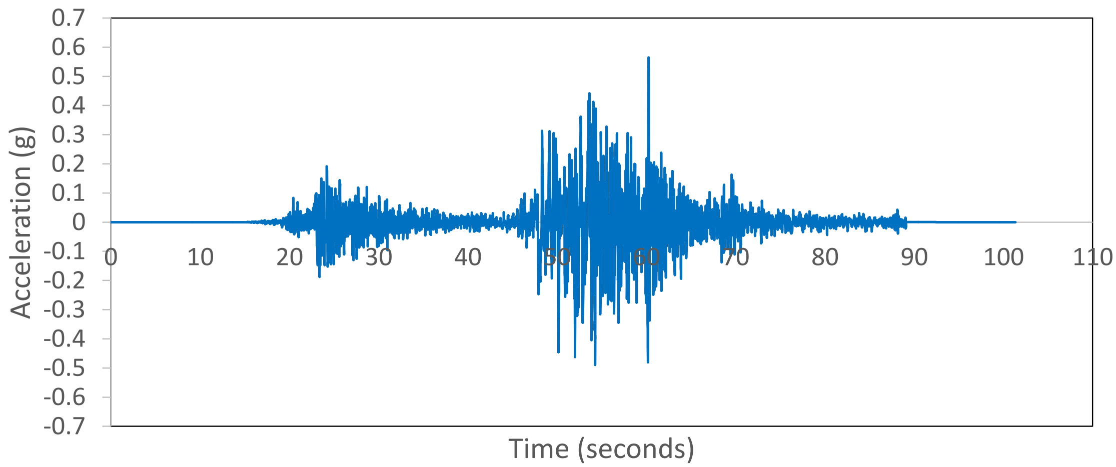

(b) NS direction accelerations versus time

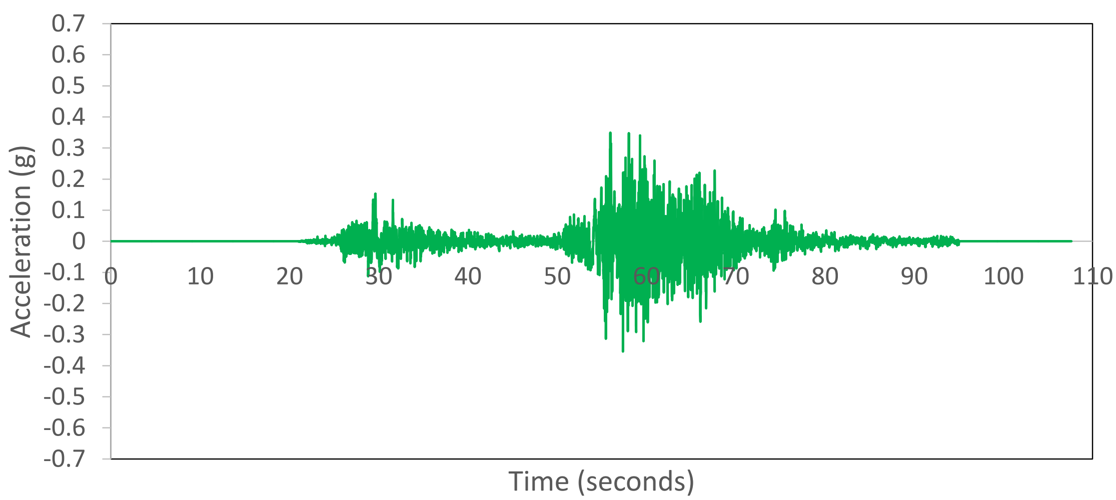

(c) Vertical direction accelerations versus time

Fig. 3-1. Station 2712 for Bridge 1, M_w 7.8 earthquake, measured accelerations in all three directions

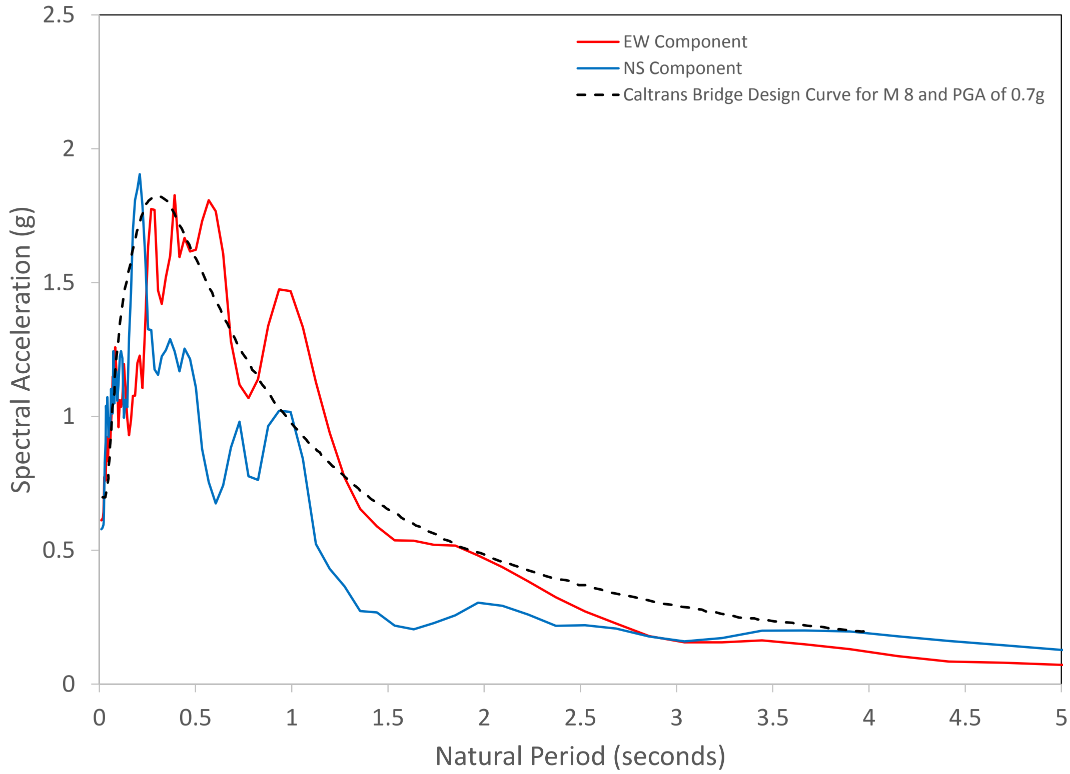

(a) EW and NS directions, as well as Caltrans Bridge Design Curve for M_w 8 earthquake with PGA of 0.7 g at a rock or stiff soil site

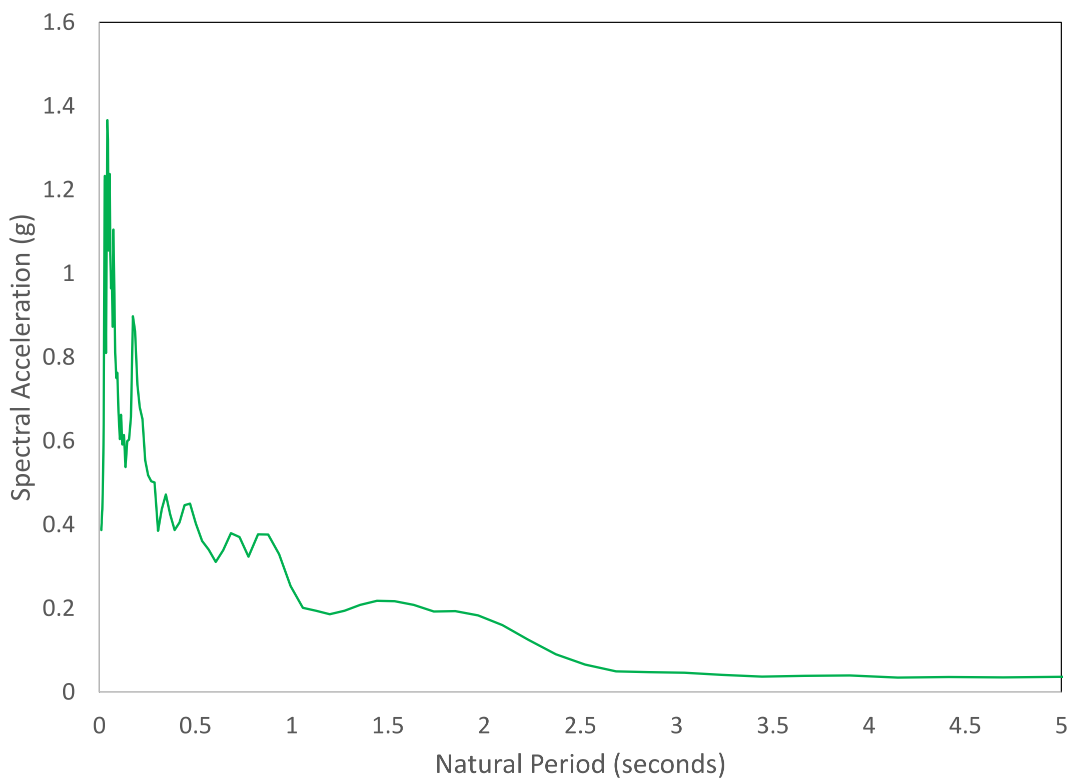

(b) Vertical direction

Fig. 3-2. Station 2712 for Bridge 1, M_w 7.8 earthquake 5% damped spectral accelerations

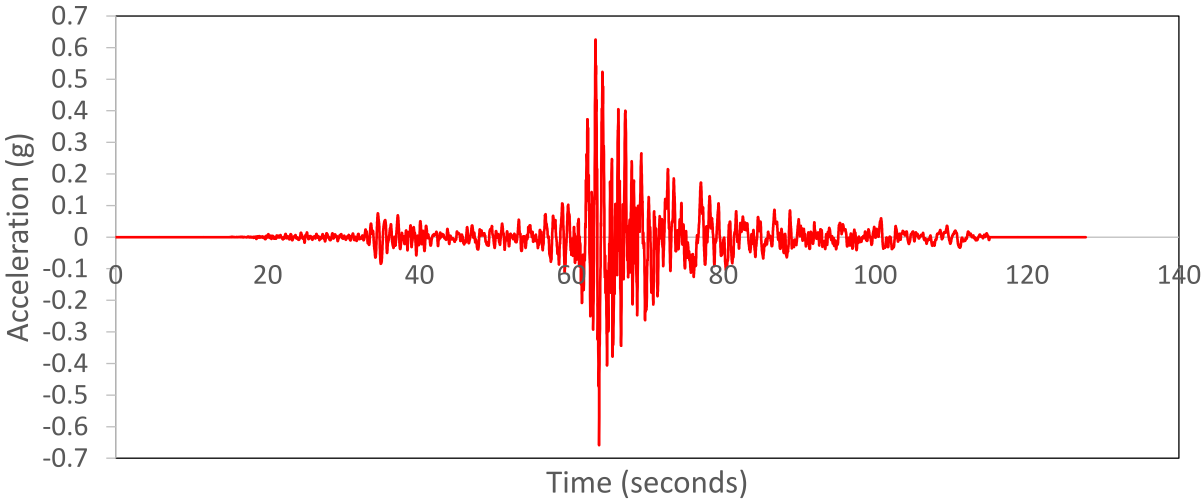

(a) EW direction accelerations versus time

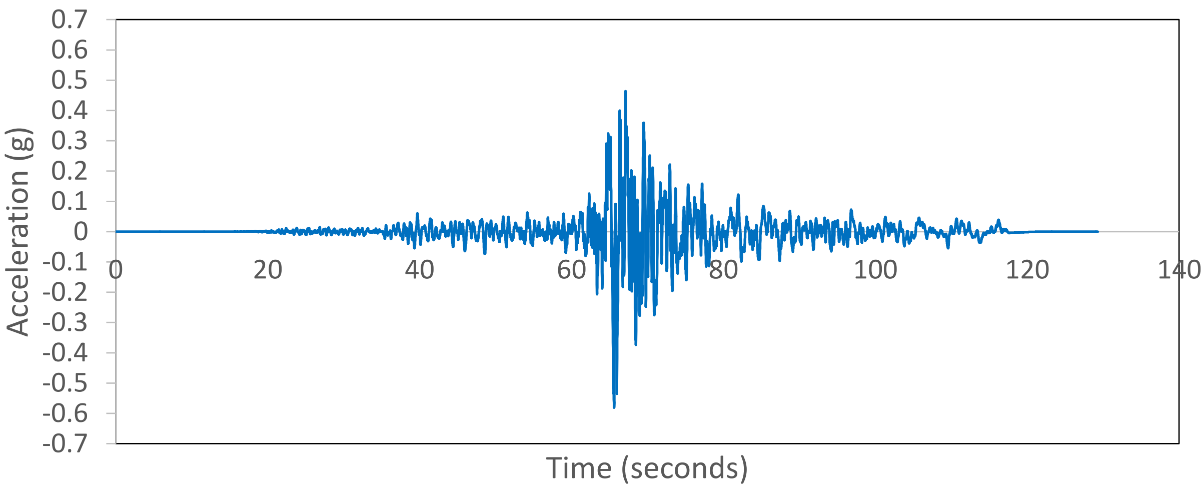

(b) NS direction accelerations versus time

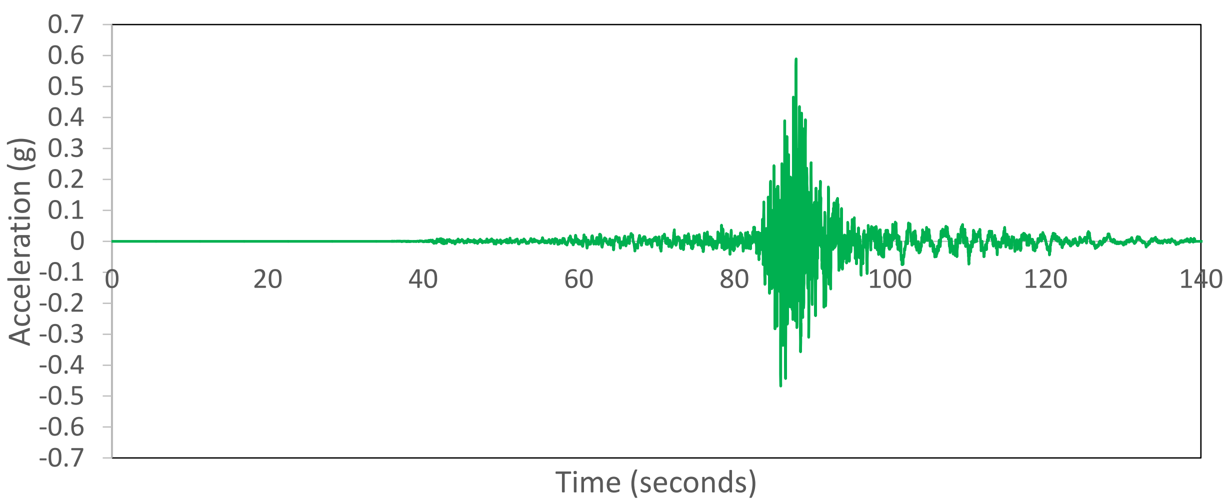

(c) Vertical direction accelerations versus time

Fig. 3-3. Station 3124 for Bridges 2 and 3, M_w 7.8 earthquake, measured accelerations in all three directions

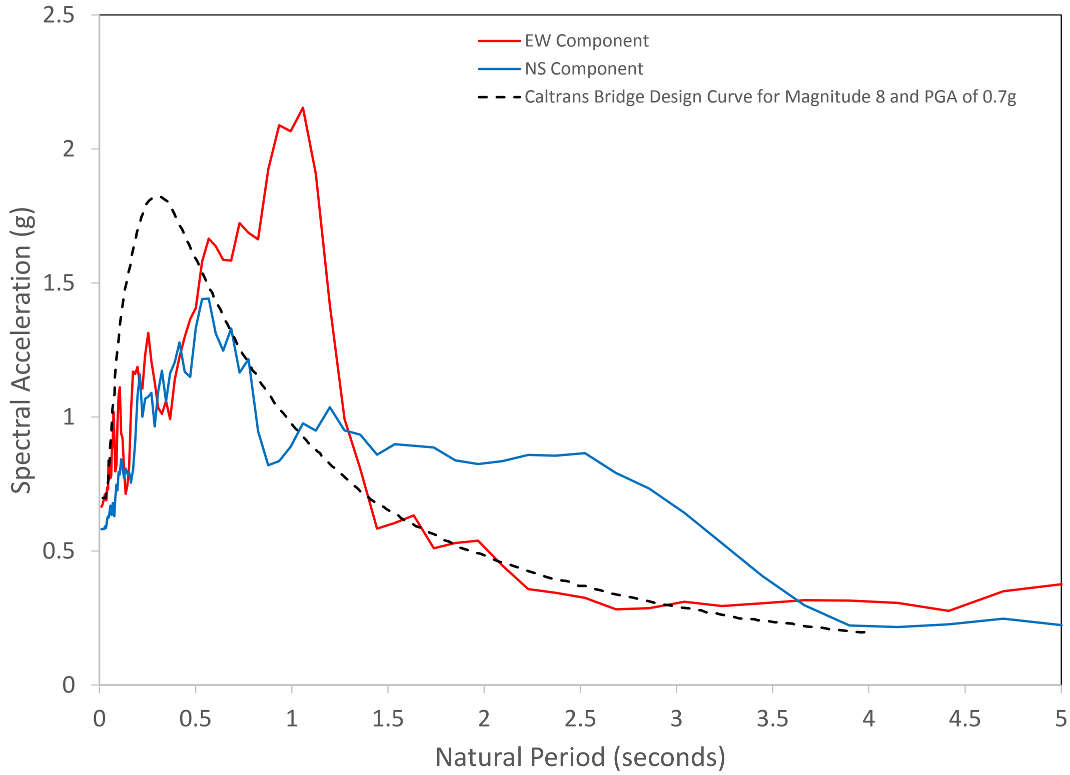

(a) EW and NS directions, as well as Caltrans Bridge Design Curve for M_w 8 earthquake with PGA of 0.7 g at a rock or stiff soil site

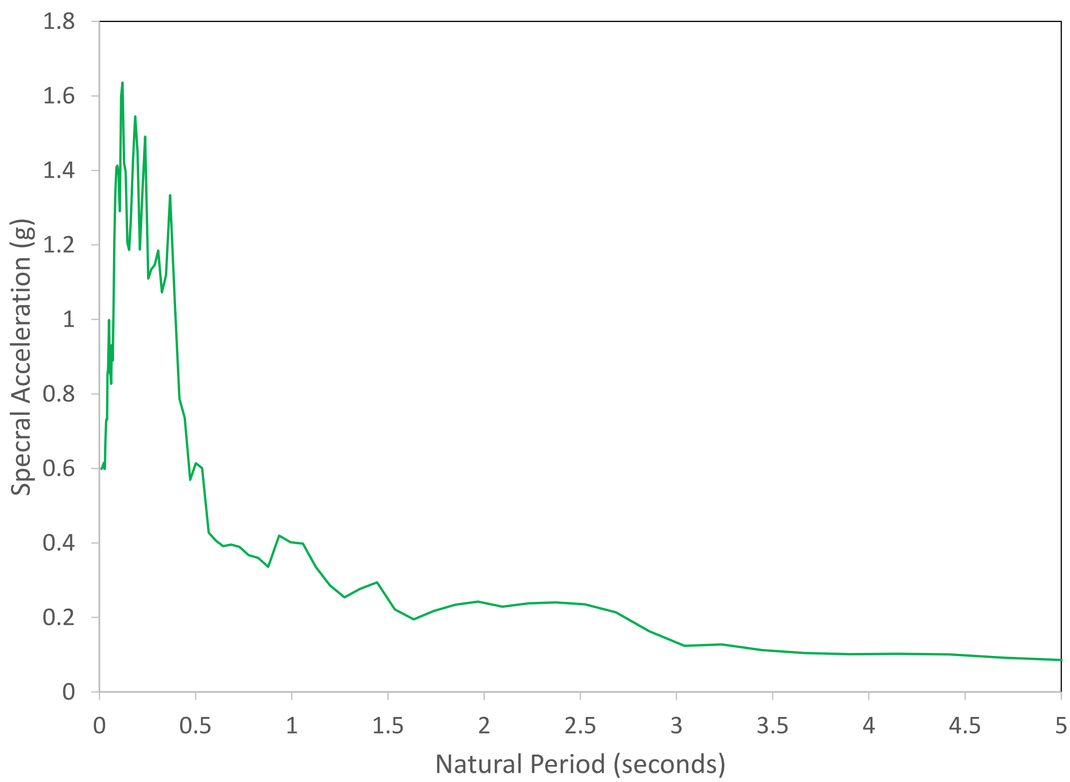

(b) Vertical directions

Fig. 3-4. Station 3124 for Bridges 2 and 3, M_w 7.8 earthquake 5% damped spectral accelerations

4. Bridge Damage

In the following three sections, three of the bridge structures that were inspected with significant and interesting damage are discussed.

4.1 Bridge 1: Five Span, Prestressed Girder/Steel Girder Superstructure with 10' Diameter RC Columns

The overall impression of the side-by-side structures of Bridge 1 (the Nurdag Viaduct), when looking at them from the above and adjacent roadway, is that they are large structures, with big and imposing circular columns of 10 foot (3.05 m) diameter and height of about 80 feet (24.4 m), with large, square, reinforced concrete (RC) footings, set in an impressive location in the low mountains, with beautiful views of pine trees close to the structures and off to the valley floor in the distance (Fig. 4.1-1). The two parallel and curved five-span bridge structures have single-column-bents with RC columns, RC footings and a combination of precast, prestressed, concrete girders (Fig. 4.1-2a) and steel box girders (Fig. 4.1-1, 4.1-2b), at GPS coordinates N 37.17096^0 E 36.69994^0 and elevation of 2563 feet (841 m). It appears that the bearings at the top of the columns may be some sort of isolation system (Fig. 4.1-1), but the bridge plans are needed before this can be verified.

Bridge 1 must have been attacked by severe ground shaking with peak spectral values in both horizontal directions exceeding the maximum Caltrans design value for a M_w 8 earthquake. And while the bridge was damaged, it remains standing, which is the design philosophy for such a large earthquake. The Caltrans bridge design curve for M_w 8 has a scatter of plus and minus M_w 0.25, indicating it is valid for M_w 7.75 to M_w 8.25, with the M_w 7.8 Turkiye earthquake being within this range. Thus the M_w 8 Caltrans seismic bridge design spectral curve is the appropriate comparison for this earthquake. It is clear that this M_w 7.8 earthquake, that so devastated southern Turkiye, is approximately equivalent to the future "Big One" in California, which has been discussed for many years in California, and elsewhere, by the media, civil engineering profession and people in general. Perhaps California and the rest of the world can now learn some lessons from what happened in Turkiye. The rupture length of 180 miles (290 km) from the M_w 7.8 event is equivalent to the distance from San Diego to Santa Barbara in California, with the City of Los Angeles (LA) right between these two cities.

Fig. 4.1-1. Overall view of bent with 10’ diameter RC bridge columns and plastic hinge for one column at about ¼ the way up its height, Bridge 1

(a) Looking toward abutments of adjacent bridges

(b) Looking toward opposite abutments of adjacent bridges

Fig. 4.1-2. Overall view of parallel and curved structures of Bridge 1

A single column plastic hinge formed at these two adjacent bridge structures of Bridge 1, but not at the bottom of the column where it is expected and detailed for, since this is where the moment is largest for a cantilever column. The plastic hinge developed in the transverse bridge direction at about ¼ up the height of the column length (Fig. 4.1-1). A side view of the plastic hinge region is given in Fig. 4.1-3. On one side of the plastic hinge the vertical column steel buckled and the transverse steel yielded over several rebar (Fig. 4.1-4), while on the opposite side a large portion of cover concrete spalled off, but with no signs of transverse steel yielding or vertical rebar buckling (Fig. 4.1-5). The most reasonable explanation for why a plastic hinge occurred 25% up the column height, instead of at the column/footing interface, as expected, is that there were vertical bar cutoffs at this location, reducing the moment capacity to the point that the moment demand/capacity ratio was larger there than at the column base (Fig. 4.1-6).

Spalling of unconfined cover concrete on both sides of this plastic hinge clearly indicates nonlinear cyclic behavior in the transverse direction of the bent, with compressive concrete strains of at least 0.005 (and probably beyond 0.01 based on the observed damage) in both loading directions [8, 11]. Vertical rebar buckling also shows that nonlinear cyclic behavior occurred, as the steel must yield and reach large strains in tension before direction reversal, which results in compressive stresses and forces in the rebar before the concrete takes any significant compression from the combined section moment and axial force. This phenomenon does not occur under monotonic loading where the concrete is always in compression on one side of the neutral axis [11].

Vertical rebar buckling in a column plastic hinge indicates that it very nearly failed, with only a couple of more cycles needed, which could have resulted in complete collapse of the structure. Note that the spacing of the transverse steel looks good (Fig. 4.1-5), but the bar size appears to be too small for a ductile plastic hinge to develop. This is probably because the plastic hinge was not expected at this location with, perhaps, larger transverse rebar provided towards the bottom of the column. While bar cutoffs is the most likely reason a plastic hinge formed part way up the column height, it is possible that this location had a larger moment demand than at the base of the column due to the combined effects of the transverse mass and rotational mass inertia from the large bridge structure, which is especially important for single-column-bent bridges [12] since the bridge is free to rotate at the top of the column in the transverse direction as it displaces transversely. Once the bridge plans are obtained, both of these possibilities can be investigated.

Depending on the size and spacing of the transverse spiral or hoops, vertical rebar can buckle between transverse bars or over many of them, which requires the transverse steel to yield and go into large tensile hoop strains, as is the case for the plastic hinge in Bridge 1. While the transverse rebar is closely spaced (Fig. 4.1-5), the size of the transverse rebar is too small to prevent buckling of the vertical rebar, with the buckled wave occurring over several transverse rebars (Figs. 4.1-3 and 4.1-4). From the author's experience, good plastic hinge performance for RC bridge columns (cyclic displacement ductility capacity of greater than six) is typically found when the volumetric ratio (percentage) of transverse rebar to the column is about one-half of the volumetric ratio (percentage) of vertical steel to the column. The required minimum amount of vertical steel for a bridge column in California is 1% [8], and so the amount of transverse steel should be at least 0.5% for good, ductile column performance. A column with more vertical steel requires more transverse rebar; for example, a column with 2% vertical steel should have about 1% transverse steel. From the images presented here, it appears that the amount of transverse steel was much less than required where the plastic hinge occurred.

Vertical rebar buckling is critical because the rebar strains (tension and compression) on both sides of a buckled wave are very large, resulting in only a few tension/compression strain cycles to cause low-cycle fatigue failure and rupture of the vertical steel. From Fig. 4.1-4, it is clear that the transverse rebar is deformed and at high strains (visibly straight on the sides of the column and tightly curved and bent around the buckled vertical steel), and once the transverse rebar ruptures the core concrete suddenly becomes unconfined, and may not be able to support even the dead load of the bridge structure, resulting in complete bridge collapse. So the combined effects of vertical rebar buckling and fracture after a few cycles, as well as yielding and rupture of transverse rebar, would not only cause the core concrete to suddenly become unconfined, it would provide the wide-open spaces required to allow this now-unconfined and crushed concrete to just pour out of the plastic hinge region. Therefore, future moderate to big earthquakes, or aftershocks, could collapse this large and important bridge structure by providing a few more cycles to the existing plastic hinge. It is of interest that in the plastic hinge region on the side of the column where the vertical bars did not buckle, the transverse rebar is seen to have constant curvature around the section with nice, even spacing (Fig. 4.1-5 and the left side of Fig. 4.1-3), and no indication of being bent out of position, as is clear on the side of the column with vertical rebar buckling (Fig. 4.1-4 and right side of Fig. 4.1-3).

In addition to the column plastic hinge discussed above, damage and spalling at the abutment from longitudinal and transverse banging of the superstructure was evident (Fig. 4.1-7).

Fig. 4.1-3. Side view of plastic hinge region of 10’ diameter RC bridge column, Bridge 1

Fig. 4.1-4. Close-up view of column plastic hinge, with buckled vertical rebar and yielded transverse rebar, Bridge 1

Fig. 4.1-5. Close-up view of column plastic hinge, spalling of cover concrete (opposite side to where vertical bars had buckled), Bridge 1

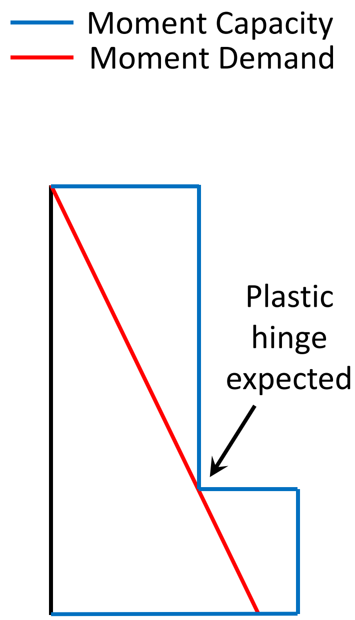

Fig. 4.1-6. Column moment demand and moment capacity when bars are cutoff at ¼ location of the column height, Bridge 1

Fig. 4.1-7. Damage at abutment, Bridge 1

4.2 Bridge 2: Six span, Precast, Pretressed I-Girder Superstructure with RC Columns

These two parallel and straight bridges are over water and located at GPS coordinates N 36.25505^0 E 36.20430^0 and elevation of 315 feet. They consist of precast, prestressed, I-girders with RC topping slab and RC columns (Fig. 4.2-1).

Fig. 4.2-1. Overall view from under Bridge 2

Lateral motion of the bridge caused severe damage and failure of external shear keys (Figs. 4.2-2 through 4.2-4). Combined lateral, longitudinal and vertical motion resulted in many rubber bearing pads that had supported the simply-supported girders to fall to the ground (Fig. 4.2-5 shows one). End regions of all of the precast concrete girders were significantly damaged from large vertical (as well as longitudinal and horizontal) accelerations and forces, including impact, resulting in shear cracks and extensive spalling of the concrete, as shown in Figs. 4.2-6 through 4.2-8. The spalling reached a long distance out into the girders (Figs. 4.2-6 and 4.2-8), far beyond the supports. In many cases there was no concrete left, with just the rebar cage remaining toward the girder end (Fig. 4.2-7) supporting the end shears. This brings up an interesting question as to what happened to the prestressing strands, and associated prestressing force, as the concrete around the strands spalled out. A coiled-up prestressing strand was found adjacent to one of the bridge abutments that had flown out of a girder (Figs. 4.2-9 and 4.2-10).

The extensive damage to the ends of both internal and external girders appears to be a result of a sequence of events; first diagonal shear cracks form just beyond the supports from large vertical accelerations and forces, including multiple impacts from girder-end liftoff and slamming back down (peak vertical spectral acceleration is 1.64 g), then concrete begins to spall off at the girder ends due to the combined effects of the large vertical, transverse and longitudinal forces, including impact in all three directions. With no concrete left at the girder ends there is nothing to hold the prestressing steel to the girder end region, with the transfer length moving forward to where there is still concrete, causing added damage to the already-cracked and spalled girder end region, with more spalling and slip, and so on, until a much longer distance of damage has developed than from just diagonal shear cracking. As seen in Figs. 4.2-6 and 4.2-8, the spalled region at the girder ends is very long for exterior girders, with similar damage occurring to interior girders (Figs. 4.2-11 through 4.2-13). Severe twisting and bending of one precast girder happened, as seen in Figs. 4.2-14 through 4.2-16.

Plastic hinges developed at the base of the columns in the longitudinal direction, which is the weak column direction (Fig. 4.2-17). Settlement occurred at both approaches to the bridge (Figs. 4.2-18 and 4.2-19), requiring vehicles to slow down to enter and exit the structure. However, traffic should not be allowed on this bridge as it is just a matter of time before complete span collapses occur from continued traffic loading and/or earthquake aftershocks due to the poor condition at all of the girder ends.

Fig. 4.2-2. Failed exterior shear keys, Bridge 2

Fig. 4.2-3. Closer view of failed exterior shear key and end-of-girder damage, Bridge 2

Fig. 4.2-4. Another view of failed exterior shear keys, Bridge 2

Fig. 4.2-5. Rubber bearing pad on ground; one of many, Bridge 2

Fig. 4.2-6. Damage to end of precast girder, Bridge 2

Fig. 4.2-7. Closer view of damage to end of precast girder, Bridge 2

Fig. 4.2-8. Damage over long range to end of exterior precast girder, Bridge 2

Fig. 4.2-9. Prestressing cable at end of precast girder, Bridge 2

Fig. 4.2-10. Close-up view of prestressing cable near end of precast girder, Bridge 2

Fig. 4.2-11. Interior girder damage at end of precast girder, Bridge 2

Fig. 4.2-12. Close-up view of interior girder damage at end of precast girder, Bridge 2

Fig. 4.2-13. Significant interior girder damage at end of precast girder, Bridge 2

Fig. 4.2-14. Significant interior girder damage at end of precast girder, Bridge 2

Fig. 4.2-15. Closer view of significant interior girder damage at end of precast girder, Bridge 2

Fig. 4.2-16. Lateral/vertical bending and damage of interior girder at mid-span and shear key damage at girder end, Bridge 2

Fig. 4.2-17. Plastic hinging at base of RC column, Bridge 2

Fig. 4.2-18. Settlement of approach to bridge, View 1, Bridge 2

Fig. 4.2-19. Settlement of approach to bridge, View 2, Bridge 2

4.3 Bridge 3: Six Span, Precast, Prestressed I-Girder Superstructure with RC Columns

These two parallel and curved bridges have six-spans with 11 precast, prestressed, I-girders per span and RC columns (Figs. 4.3-1 and 4.3-2), located at GPS coordinates N 36.24060^0 E 36.21406^0 and elevation of 336 feet. Damage observed for Bridge 3 includes cracking and spalling at the ends of the precast girders (Figs. 4.3-3 and 4.3-4), as well as failure of external (Fig. 4.3-5) and internal shear keys (Fig. 4.3-6). The maximum vertical acceleration recorded for this bridge was 0.589 g, with peak vertical spectral acceleration of 1.64 g. This indicates that the shear forces at the ends of the simply-supported precast girders were much larger than from just the static dead load of the structure, and that the girders were lifting off of the supports and slamming back down, resulting in impact shear forces that were larger than the girders were designed for, causing the shear cracking and concrete spalling seen at the girder ends (Figs. 4.3-3 and 4.3-4), which is similar to, but not as severe as, what was observed at Bridge 2.

Fig. 4.3-1. Overall view of Bridge 3

Fig. 4.3-2. View under Bridge 3, showing 11 precast I-girders per span for each bridge

At the same time that the girders were being lifted off of their seats and slammed back down again, large horizontal and longitudinal forces were occurring, adding to the damage at the girder ends, and causing the shear key damage and failures that were observed (Figs. 4.3-5 and 4.3-6). Since the precast girders are only connected to each other through the cast-in-place (CIP) topping slab, they are free to move about almost independently of each other away from the deck. Adding at least one diaphragm along the length of each span would have helped the bridge move as a unit rather than as independent precast girders, which would have been even more important for Bridge 2.

Fig. 4.3-3. Damage at end of Bridge 3 precast girders

Fig. 4.3-4. Close-up view of damage at end of Bridge 3 precast girder

Fig. 4.3-5. Damage of external shear key at Bridge 3 abutment

Fig. 4.3-6. Damage of internal shear key at bent of Bridge 3

5. Conclusions

The team spent six days in the field inspecting residential buildings, bridges, silos, mosques, churches, industrial buildings and schools for structural damage and failure, starting two weeks after the M_w 7.8 and M_w 7.5 earthquakes that occurred in southern Turkiye on February 6, 2023. The team visited Iskenderun, Antakya, Osmaniye, Kahramanmaras, Gaziantep, Nurdagi, Golbasi and Hatay, traveling to the field each day by vehicle from Adana, and returning to Adana each evening. Most residential building failures, and related deaths, occurred in a particular type of construction that is used throughout Turkiye consisting of a RC frame of columns and girders, and infill walls of bricks or masonry blocks, with no gaps between the walls and the frame.

The infill walls are not connected to the frame members and the bricks, or masonry blocks, are not tied to each other. Because of this, the infill walls are not considered in seismic design as part of the lateral load-resisting system. However, as the diagonal shear cracks seen on almost all infill walls for most of these buildings clearly demonstrate, these walls *are* resisting lateral loads before they fail and (partially or fully) fall out, forcing the RC frame to suddenly take all of the earthquake loads. The combined response of frame and infill walls is much stiffer than the frame acting by itself, causing amplification of the earthquake loads above what is considered in design, leading to failure of these building types. Infill walls can also cause a short column effect, with larger shears than expected from the full column length assumption. In addition, the team noticed column failures from cracked and damaged infill walls pushing into them. Many building failures were also due to soft soil and liquefaction of sandy soils, and related settlement, with some building structures rotating as a unit about their foundations. Sand boils, liquefaction, lateral spreading, settlement and multiple wide-open, deep cracks in the soil were seen in several locations.

While tens of thousands of residential buildings collapsed (responsible for most of the deaths from this natural/man-made disaster), as did various mosques, churches, silos and industrial buildings, there were no bridge failures as far as the team is aware. Several bridge structures had severe damage, as expected under such an extreme event, but they remained standing, which is consistent with modern seismic design philosophy; allow extensive damage but no collapse in order to save lives. This demonstrates that it is possible to design and build civil engineering structures that do not collapse from large earthquakes. While RC buildings with infill walls failed in almost unbelievable numbers, some were heavily damaged but remained standing, with girder and column plastic hinges in critical locations properly forming. Prior to rebuilding, Turkiye needs to consider changes to this type of building structure.

If a similar type of building is used, infill walls must be connected to the frame members and a gap provided to allow the columns and girders to bend and form plastic hinges where they are designed and detailed to occur for seismic loading. Bricks and masonry blocks must also be connected to each other to prevent them from falling to the street below or into the apartments. Base isolation for new and existing structures of Turkiye should be considered, since this will remove almost all lateral seismic forces from the structure, with the building virtually decoupled from the ground. All of the structures that the team is aware of that were built on base isolation performed well, with no collapse and no damage. This is especially important when considering Istanbul, with about 15 million people living in similar buildings that collapsed in southern Turkiye.

This report presented findings from three observed bridge structures that were damaged but remained standing. The team is not aware of any bridge structures that collapsed from the earthquake sequence that occurred in southern Turkiye on February 6, 2023.

6. References

1. USGS (2023a). https://earthquake.usgs.gov/earthquakes/eventpage/us6000jllz/executive
2. USGS (2023b). https://earthquake.usgs.gov/earthquakes/eventpage/us6000jlqa/executive
3. Hancilar, U., Sesetyan, K., Cakti, E., Safak, E., Yenihayat, N., Malcioglu, F. S., Donmez, K., Tetik, T., Suleyman, H. (2023). Kahramanmaraş-Gaziantep Türkiye M7.7 Earthquake, 6

February 2023 (04:17 GMT+03:00) Strong Ground Motion and Building Damage Estimations Preliminary Report (v6)

4. Cetin et al. (2023). Preliminary Reconnaissance Report on February 6, 2023, Pazarcık M_w=7.7 and Elbistan M_w =7.6, Kahramanmaraş-Türkiye Earthquakes. METU Earthquake Engineering Research Center.

5. 50 Years Later, an Earthquake's Legacy Continues, USGS, Communications and Publishing, 2021.

6. Competing Against Time: Report to Governor Deukmejian from the Governor's Board of Inquiry on the 1989 Loma Prieta earthquake, 1989.

7. The Continuing Challenge: Report on the Northridge Earthquake to the Director, Department of Transportation, State of California, by the Seismic Advisory Board, 1994.

8. Caltrans Seismic Design Criteria (SDC), Version 2.0, 2019.

9. TEBC (2019). Turkish Building Earthquake Code; *T.C. Resmi Gazete:* Ankara, Turkey.

10. Caltrans Seismic Design Criteria (SDC), Version 1.4, 2006.

11. Priestley, M.J.N., Seible, F., & Calvi, G.M., Seismic Design and Retrofit of Bridges, John Wiley and Sons, New York, 1996.

12. Dowell, R.K., Time-History Analyses versus Measured Seismic Responses of the 5/14 Connector Bridge, Report (# DH-04-02) to the Strong Motion Instrumentation Program, California Geological Survey, from Dowell-Holombo Engineering, 2004.